



Preparation and Characterization of a W/O Composite Camellia Microemulsion for Cosmetic Applications

Yao Qin, Jingru Qian, Bingqing Yu, Jialei Yan, Yiyi Peng, Jianming Wang, Tingzhi Zhang, Jing Wang

Syoung Cosmetics Manufacturing Co., Ltd., Changsha 410006, Hunan, China

Abstract: Camellia seed oil (CA) is a promising cosmetic raw material with excellent antioxidant and reparative properties. In this study, a W/O composite camellia microemulsion (CCME) was prepared using a mixture of camellia seed oil and surfactants (soy lecithin and dipropylene glycol, $K_m=2.5:1$) at a 5:5 ratio. The physicochemical properties were investigated, including average particle size, zeta potential, and storage stability. DLS results showed that the values of the average particle size and the polydispersity index (PDI) for the obtained CCME prepared under the optimized conditions were $68.96\pm2.91\text{ nm}$ and 0.267 ± 0.015 . The formulation exhibited excellent centrifugal and static stability, facilitating its application in cosmetic products. Compared to pure camellia seed oil, the composite camellia microemulsion showed significantly higher DPPH radical scavenging capacity ($88.25\pm2.13\%$, $P < 0.05$). In skin-soothing efficacy tests using a 3D skin model, the composite microemulsion demonstrated superior repair effects over camellia seed oil. Further verification revealed that this enhanced reparative performance may be attributed to its upregulated expression of skin barrier structural proteins such as loricrin (LOR). In conclusion, the composite camellia microemulsion developed in this work exhibits favorable application potential and efficacy, indicating its significant benefits for cosmetic applications.

Keywords: camellia seed oil; microemulsion; W/O; skin permeation; transdermal delivery; skin barrier repair; cosmetics

1. Introduction

Camellia seed oil (CA) extracted from the seeds of Camellia plants, shares a similar fatty acid profile with olive oil and is often hailed as the “Oriental Olive Oil” [1]. Rich in oleic acid, linoleic acid, triglycerides, and bioactive compounds like camelliaside, tea polyphenols, phospholipids, saponins, tannins, phytosterols, natural tocopherols, and squalene, CA exhibits potent antioxidant, anti-inflammatory, reparative, and whitening effects, making it a valuable cosmetic ingredient [2-4]. Eunsun Jung revealed through in vitro studies that camellia oil inhibits matrix metalloproteinase-1 (MMP-1) activity while simultaneously inducing human type I procollagen synthesis, with clinical trials further validating its skin barrier repair efficacy [5]. However, challenges like low solubility in aqueous phases, oxidation susceptibility, and potential precipitation of saturated fatty acids at low temperatures (common in refined grades) limit its broader cosmetic application [6].

Camellia japonica flower extract contains active compounds such as polysaccharides, polyphenols, flavonoids, and vitamin C, which exhibit strong antioxidant capacity and offer protective effects against urban air pollutant-induced skin aging mechanisms. Amorepacific Corporation investigated the antioxidant activity of red camellia extract and examined the MMP-1 inhibitory effects of kaempferol triglycoside and tetraglycoside derived from it [7]. Microemulsions are thermodynamically stable, transparent (or translucent), low-viscosity systems formed from water, oil, surfactant, and cosurfactant in specific ratios [8,9]. Their unique structure enables the solubilization of poorly water-soluble or incompatible substances, enhancing synergistic effects. Crucially, microemulsions have been proven superior to simple solutions or traditional formulations in enhancing the skin permeation of cosmetic actives and drugs by overcoming the barrier function of the stratum corneum [10]. To overcome these limitations and enhance the functional benefits of CA, this study integrated CA with complementary hydrophilic actives, namely Camellia japonica flower extract and madecassoside, utilizing microemulsion technology.

Research on Camellia-based systems in cosmetics remains limited. To broaden the application scope and enhance the efficacy of CA in skincare, this study employed microencapsulation technology. A W/O CCME was developed by combining hydrophilic actives (Camellia japonica flower and madecassoside) with lipophilic CA. This approach aimed to (1) improve the stability of CA and enhance its capacity to encapsulate hydrophilic active components, (2) utilize the nanocarrier system to enhance the penetration of CA through the stratum corneum, (3) leverage the synergistic interactions among CA, Camellia japonica flower and madecassoside to boost antioxidant and soothing efficacy, thereby enhancing overall skincare value.

2. Materials and Methods

2.1 Design and Preparation of W/O Composite Camellia Microemulsion

Soybean lecithin was selected as the surfactant and dipropylene glycol (DPG) as the cosurfactant based on pre-screening. CA (Zhina Biotechnology Co., Ltd., Shanghai, China) served as the oil phase. The aqueous phase consisted of a 5:1 (w/w) mixture of camellia japonica flower (BioSpectrum Inc., Korea) and madecassoside (SEPPIC, France). The surfactant-to-cosurfactant mass ratio (Km) was fixed at 2.5:1. The microemulsion formation region was investigated by varying the oil-to-surfactant mixture mass ratio (Oil/Smix) from 0:10 to 10:0. The oil phase and the surfactant/cosurfactant mixture were homogenized using a magnetic stirrer. Distilled water was titrated dropwise into the mixture. The transition points from turbidity to clarity were recorded, noting the composition at each point. A pseudo-ternary phase diagram (water, oil Smix) was constructed using Origin Pro 8.5 software to identify the optimal microemulsion region.

Based on the phase diagram, the microemulsion was prepared. Precisely weighed soybean lecithin (35 g), DPG (14 g), and CA (50 g) were mixed in a 100 mL beaker. Under magnetic stirring at 650 rpm and 80–90 °C, the pre-mixed aqueous phase (camellia japonica flower/madecassoside = 5:1) was added dropwise until a clear, transparent CCME was obtained.

2.2 Physicochemical Characterization

Particle Size and Zeta Potential: Freshly prepared CCME samples were diluted appropriately. The average particle size, polydispersity index (PDI), and zeta potential were measured using a dynamic light scattering (DLS) instrument at a scattering angle of 90° and a temperature of 25 °C. Measurements were performed in triplicate.

Morphological Observation: Freshly prepared CCME was diluted. A drop of the diluted sample was placed on a carbon-coated copper grid and air-dried. The sample was then negatively stained with 2(wt)% phosphotungstic acid solution and air-dried again before observation under a transmission electron microscope (TEM).

2.3 Stability Studies

(1) **Centrifugal Stability:** Freshly prepared CCME (5 mL) was placed in a 10 mL centrifuge tube and centrifuged at 4000 rpm and 25 °C for 10, 20, 30, and 40 min. The samples were visually inspected for phase separation. If no separation occurred, the average particle size and PDI were measured. The centrifugal stability parameter (KE) was calculated using the formula:

$$K_E = \frac{R_0 - R}{R_0} \times 100\% \quad (1)$$

R₀ is the particle size before centrifugation; R is the particle size after centrifugation.

(2) **Storage Stability:** Freshly prepared CCME was stored in sealed containers at room temperature (RT, 20 °C), elevated temperature (45 °C), and low temperature (4 °C). Samples were visually inspected for phase separation at 7, 14, 28, 35, 42, and 56 days. If no separation occurred, the particle size and PDI were measured.

2.4 Transdermal Penetration Testing

(1) **In Vitro Permeation Test:** Franz diffusion cells (diffusion area: 2.27 cm², receptor volume: 7.0 mL) were used. The apparatus temperature was maintained at 37.0 ± 0.2 °C with a stirring speed of 400 rpm. Excised Bama pig skin was mounted between the donor and receptor compartments, with the stratum corneum facing the donor chamber. The receptor chamber was filled with PBS buffer, ensuring no air bubbles trapped between the skin and the receptor fluid. The donor chamber was loaded with 7 mL of the sample (CCME or CA). Samples permeating through the skin into the receptor chamber were collected at 0.5, 1, 2, 4, 6, 8, and 12 h. The concentrations of the analytes in the receptor fluid and within the skin were determined. The cumulative amount permeated per unit area (Q_n, µg/cm²) was calculated as:

$$Q_n = (C_n V_s + \sum_{i=1}^{n-1} C_i V) / S \quad (2)$$

C_n is the concentration at the nth sampling point, C_i is the concentration at the ith sampling point, V_s is the volume of the receptor chamber, V is the volume of sample withdrawn, S is the effective diffusion area.

(2) **In Vivo Human Permeation Test:** Five healthy volunteers (aged 18–60 years) were enrolled according to inclusion criteria. Written informed consent was obtained prior to testing, following the Declaration of Helsinki. Before testing, both forearms were washed with water. Volunteers acclimatized for 30 min in a controlled environment (22 ± 1 °C, 55% ± 5% RH). Four 4 cm × 4 cm test areas were marked on the inner forearms. Confocal Raman spectroscopy (CRS) was used to measure the baseline stratum corneum thickness. CCME was applied to the test areas. The penetration depth and relative

amount of active components within the stratum corneum were measured by CRS at baseline, 0.5 h, 2 h, 3 h, 6 h, and 12 h post-application. Measure five points in each area, in triplicate.

2.5 Antioxidant Activity Test

A DPPH stock solution (4 mg in 50 mL ethyl acetate) was prepared and stored protected from light at low temperature. Test solutions were added to a 96-well plate as follows:

Control Group (A1): 100 μ L DPPH solution + 100 μ L water.

Sample Group (A2): 100 μ L sample solution + 100 μ L DPPH solution.

Blank Group (A3): 100 μ L sample solution + 100 μ L ethyl acetate.

The plate was incubated in the dark at room temperature for 30 min. The absorbance at 517 nm was measured (A1, A2, A3). Tests were performed in triplicate. The DPPH radical scavenging rate (SE, %) was calculated as:

$$S_E = \frac{A1 - (A2 - A3)}{A1} \times 100\% \quad (3)$$

2.6 Skin Barrier Repair Efficacy Testing

(1) 3D Skin Model Repair Test: An in vitro 3D skin damage model was established using sodium lauryl sulfate (SLS) as the irritant on a reconstructed human epidermis model. After applying the test samples to the damaged model, it was incubated at 37 °C and 5% CO₂ for 24 h. Skin barrier repair efficacy was assessed by comparing the density of the stratum corneum structure via hematoxylin and eosin (HE) staining. Groups included: Blank Control (BC, untreated), Positive Control (PC, Pirfenidone), CCME, and CA.

(2) Expression of Skin Barrier Structural Protein (LOR): HaCaT cells were seeded in 96-well plates at 15,000 cells/well and cultured for 24 h (37 °C, 5% CO₂). When cell confluence reached 40–60%, treatments were applied according to the experimental design. After 24 h incubation, LOR content was measured. The medium was aspirated, cells were washed with PBS (3 × 300 μ L/well), fixed with 4% paraformaldehyde (100 μ L/well, 20 min, RT), and washed again with PBS (5 × 300 μ L/well). Cells were permeabilized with 0.1% immunostaining permeabilization buffer (100 μ L/well) and washed (5 × 300 μ L/well). Non-specific binding was blocked with 5% FBS (100 μ L/well, 1 h, RT). After aspiration, cells were incubated overnight at 4 °C in the dark with primary antibody against LOR (diluted 1:50 in antibody dilution buffer, 50 μ L/well). Cells were warmed to RT for 30 min, washed (3 × 5 min, 300 μ L/well), incubated with fluorescently labeled secondary antibody (diluted 1:200 in antibody dilution buffer, 50 μ L/well, 1 h, RT, dark), and washed again (3 × 300 μ L/well). Cells were kept in 50 μ L PBS/well and imaged under a fluorescence microscope. The average fluorescence intensity (MFI) was quantified using ImageJ software. Groups included: Blank Control (BC, medium only), Negative Control (NC, MEM medium), Positive Control (PC, EGCG), CCME, and CA.

3. Results

3.1 Construction of the Pseudo-Ternary Phase Diagram

Soybean lecithin, a biocompatible nonionic surfactant, was chosen for its ability to lower interfacial tension and enhance skin affinity and permeation. DPG was selected as the cosurfactant for its role in stabilizing microemulsions and its permeation-enhancing properties [11–13]. This optimized combination aimed to improve the bioavailability of CA and *Camellia japonica* flower.

The pseudo-ternary phase diagram of the CA system (Figure 1) revealed the largest microemulsion region (12.82%) at Km = 2.5:1. The chosen composition maximized water content for applicability while minimizing surfactant concentration to reduce potential toxicity. Higher water content also contributed to lower viscosity, facilitating efficient and uniform application on the skin, counteracting the thickening effect of higher lecithin content. Consequently, an oil-to-surfactant mixture ratio of 5:5 was selected for preparing the W/O CCME. Although termed ‘microemulsion’ for consistency with cosmetic nomenclature, the system requires energy input (heating/stirring) suggesting nanoemulsion-like behavior.

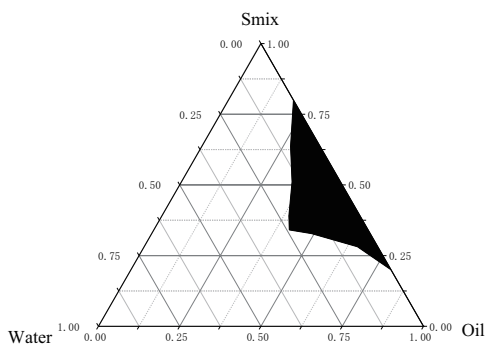


Figure 1. Pseudo-ternary phase diagram of microemulsions composed of Camellia seed oil (oil phase), surfactant mixture (Smix, soybean lecithin and DPG = 2.5:1), and aqueous phase (Camellia japonica flower extract and madecassoside = 5:1).

3.2 Physicochemical Properties of the CCME

The CCME appeared as a pale yellow, clear liquid. DLS analysis showed an average particle size of 68.96 ± 2.91 nm, a PDI of 0.267 ± 0.015 , and a zeta potential of -13.62 ± 0.57 mV (Figure 2a). The sub-100 nm size and moderate negative surface charge, coupled with a PDI < 0.4 , indicated a narrow size distribution, good homogeneity, and favorable stability.

Morphological analysis of the freshly prepared CCME was performed using transmission electron microscopy (Figure 2b). Spherical particles with uniform size distribution were observed, indicating favorable microscopic morphology of the composite camellia seed oil microemulsion. The particle size was approximately 150 nm, showing an increase compared to DLS measurements. This discrepancy may be attributed to dehydration-induced structural changes: soy lecithin under TEM vacuum conditions, causing folding of hydrophobic chains and subsequent apparent size expansion. Additionally, rapid freezing during sample preparation may promote aggregation of the oil phase (CA), magnifying the measured dimensions [14].

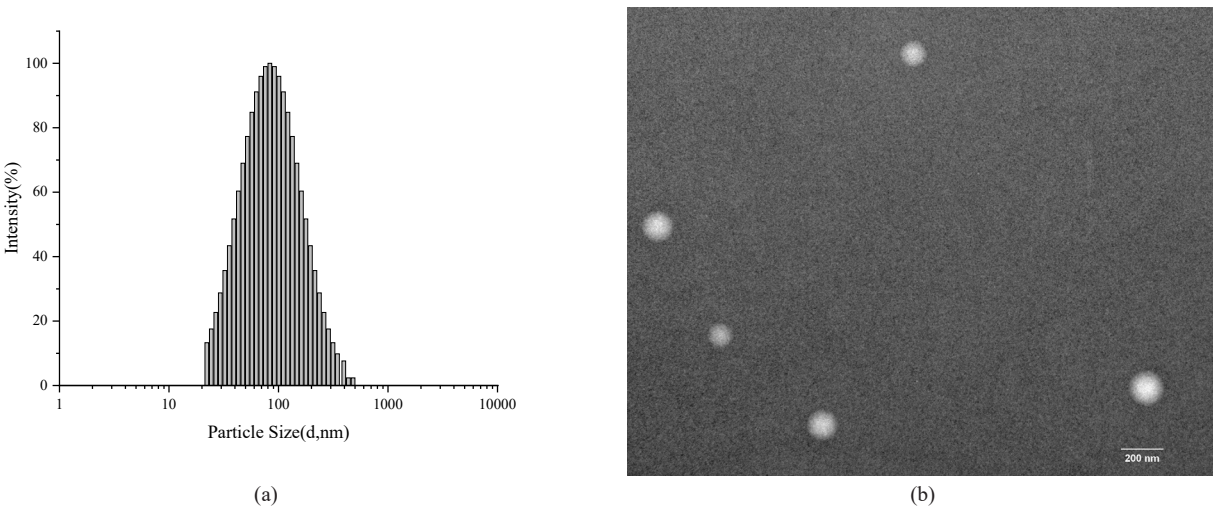


Figure 2. (a) Particle size distribution, (b) TEM image of the CCME.

3.3 Stability of the Composite Camellia Microemulsion

Considering the practical application of the CCME in cosmetics, its stability under conditions simulating transportation, usage, and storage was evaluated through centrifugation and long-term storage tests.

Centrifugal stability simulates conditions during transportation. No precipitation or phase separation occurred in the samples centrifuged at 4000 rpm for different durations (Figure 3). The changes in average particle size were minimal, and the centrifugal stability parameter KE was consistently less than 5%, indicating excellent centrifugal stability.

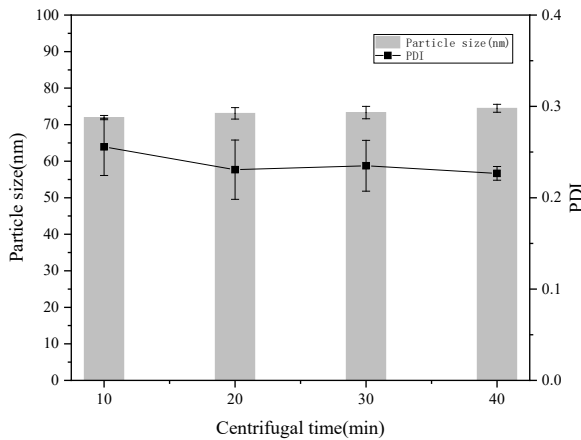


Figure 3. Changes in particle size and PDI of the microemulsion over different centrifugation times.

Long-term storage can lead to nanoparticle aggregation, size increase, and even phase separation. The stability of the CCME stored at high temperature (45 °C), room temperature (20 °C), and low temperature (4 °C) for 8 weeks was investigated. Changes in average particle size and PDI are shown in Figure 4. The particle size and PDI changed minimally at RT and 45 °C, remaining within the range of 60–80 nm. At 4 °C, a slight increase in particle size was observed, from 68.96 ± 0.91 nm to 92.64 ± 1.48 nm, but no phase separation occurred. Overall, the prepared CCME exhibited excellent stability for practical application, transportation, and storage.

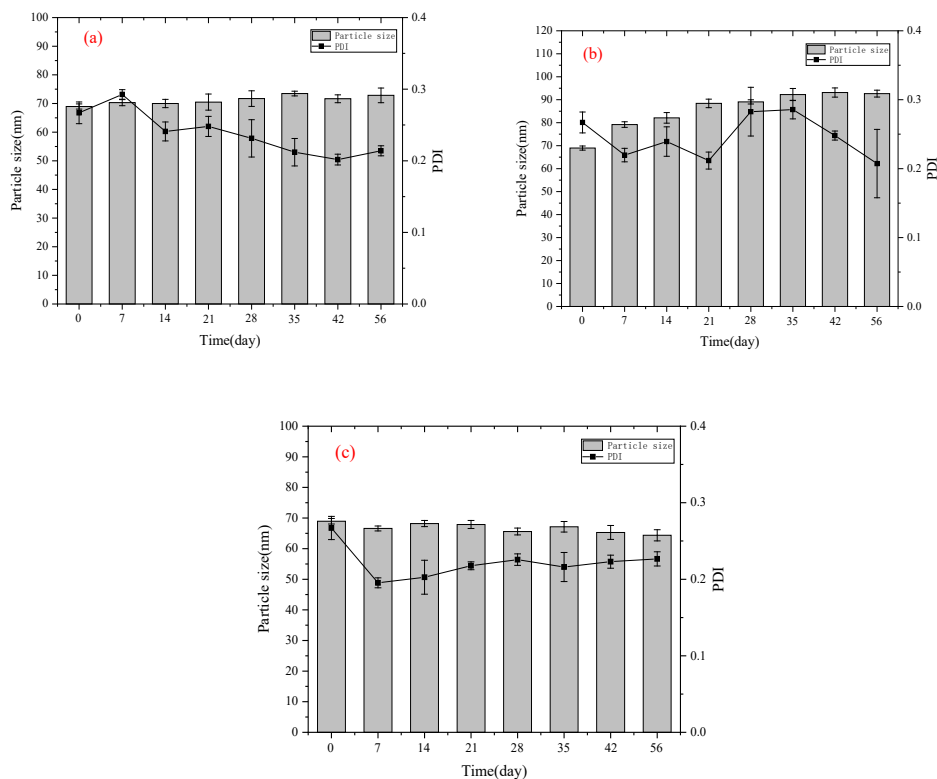


Figure 4. Changes in particle size and PDI of the microemulsion over time at different storage temperatures:
(a) Room temperature, (b) Low temperature (4 °C), (c) High temperature (45 °C).

3.4 Results of Transdermal Absorption Testing

The stratum corneum presents a significant barrier to the penetration of topically applied cosmetics or drugs. Nano-scale microemulsions can enhance the transdermal absorption of lipophilic drugs by increasing their solubility, thermodynamic

activity, and altering their affinity for the internal phase [9,15,16]. To verify this, the in vitro permeation ability of the prepared CCME was compared with that of pure CA. The results (Figure 5) showed that initially, due to the barrier effect of the stratum corneum, neither CA nor CCME penetrated the skin. The cumulative amount permeated per unit area (Qn) of CCME increased significantly over time. This superior permeation performance compared to pure CA is attributed to the smaller particle size of the CCME and the penetration-enhancing effect of the surfactant complex in the formulation.

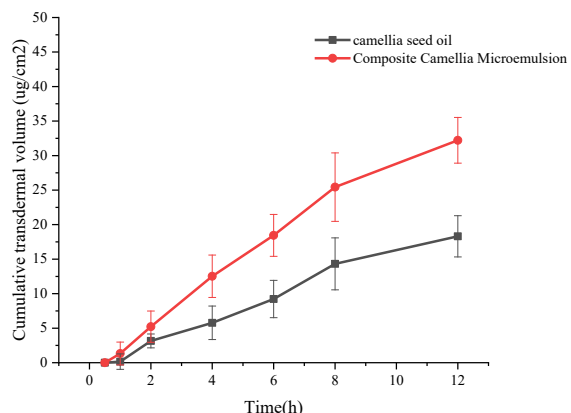


Figure 5. Cumulative skin permeation amounts of the CCME and CA.

To validate its actual penetration performance in human application, we further assessed the penetration rate over 12 hours on the human forearm using confocal Raman spectroscopy (CRS). The inner forearm is a common site for transdermal penetration studies. To ensure scientific validity, five volunteers participated in a pre-test. CRS was used to study changes in skin lipid structure and the amount of drug penetrating into the stratum corneum after application, evaluating the penetration-enhancing effect. Three parallel test areas per volunteer were used.

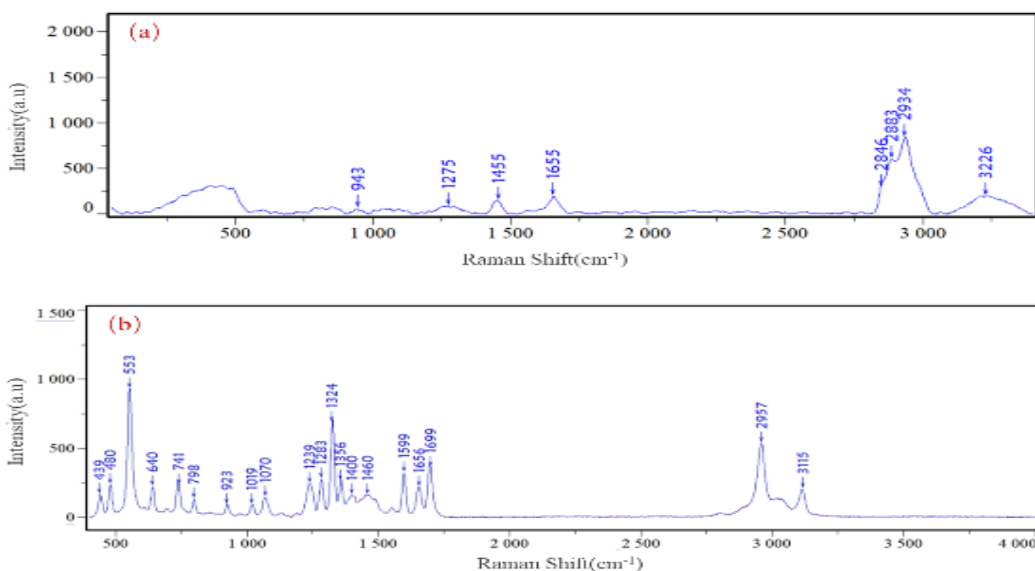


Figure 6. Raman spectra: (a) Human skin, (b) CCME.

The Raman signal of the CCME was detected using the confocal Raman spectrometer and compared with that of human skin. Characteristic peaks at 553 cm^{-1} , 1324 cm^{-1} , and 1699 cm^{-1} were ultimately selected to track the penetration depth and relative amount of components within the skin layers.

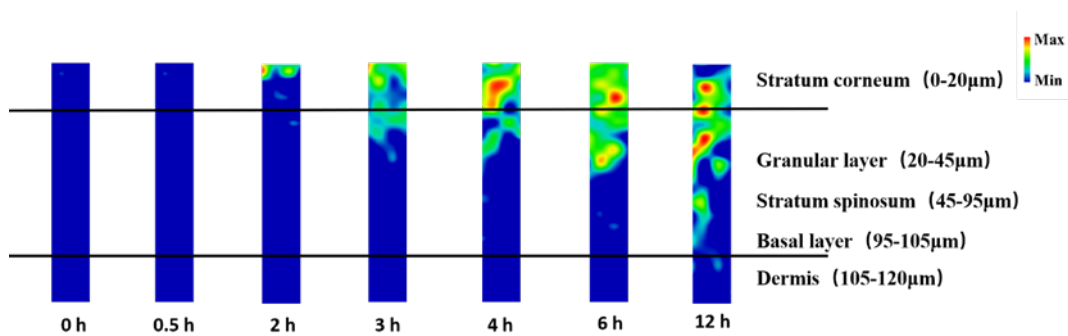


Figure 7. In vivo human Raman penetration images of the CCME.

The average baseline stratum corneum thickness of the volunteers' inner forearms was approximately 20 μm . Figure 7 shows the penetration results of the CCME on human skin. After a single application, measurements were taken at the test sites at 0.5 h, 2 h, 3 h, 4 h, 6 h, and 12 h. The calculated relative penetration rates were 0.11%, 1.38%, 4.49%, 6.37%, 9.68%, and 12.02%, respectively. These results indicate good retention after application. Over time, the CCME continuously penetrated the stratum corneum, accumulated in the viable epidermis, moved towards the dermis, acted on intercellular skin cells, and improved its bioavailability.

3.5 Results of Antioxidant Activity Test

The DPPH radical scavenging assay is a rapid and simple in vitro method for evaluating antioxidant activity. When a radical scavenger is present in solution, DPPH combines with it, causing the purple color to fade and the absorbance at 517 nm to decrease linearly with the amount of DPPH scavenged [17,18]. As shown in Table 1, CA exhibited good antioxidant activity. However, the CCME demonstrated significantly higher antioxidant activity compared to pure CA. This enhancement is attributed to the synergistic effect of protocatechuic acid and other antioxidants present in the encapsulated *Camellia japonica* flower extract, which collectively increased the DPPH scavenging rate.

Table 1. DPPH free radical scavenging rate of different samples.

Sample	Scavenging Rate (%)
Camellia Seed (CA)	65.85 \pm 1.45
Camellia japonica Flower Extract	18.95 \pm 1.17
Composite Camellia Microemulsion (CCME)	88.25 \pm 2.13

3.6 Results of Skin Barrier Repair Efficacy Testing

To comply with the EU ban on animal testing for cosmetic ingredients and finished products, a 3D skin model was utilized for in vitro efficacy assessment of cosmetic ingredients. The primary indicator of barrier repair efficacy is the density of the stratum corneum structure, followed by its thickness. A denser stratum corneum indicates better barrier repair [19].

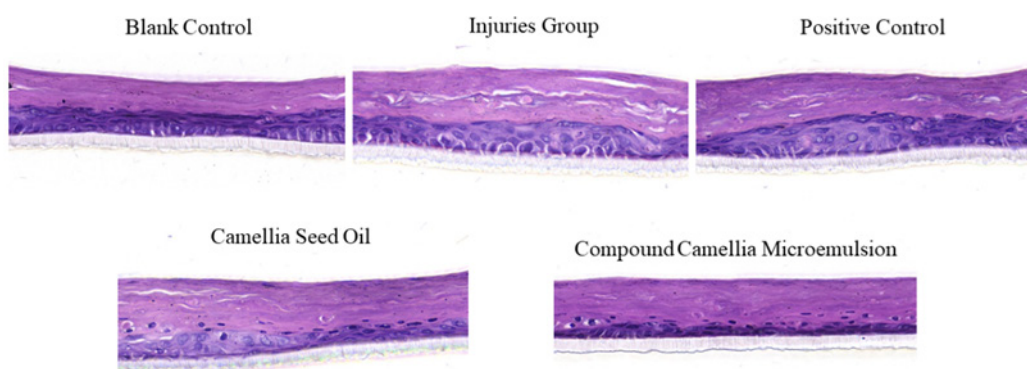


Figure 8. Staining images showing the barrier repair effects of different samples on 3D skin models. Groups: Blank Control (BC), Positive Control (PC, Pиренидон), Camellia seed oil (CA), Composite Camellia Microemulsion (CCME).

SLS an anionic surfactant widely used in skincare products like soaps and shampoos, damages the skin by disrupting the integrity of the stratum corneum. Severe damage to the skin model by SLS was observed (Figure 8). After damage, application of 0.4% CA resulted in a slightly denser stratum corneum compared to the positive control (PC, Pиренидон).

Strikingly, application of 0.4% CCME resulted in a significantly denser stratum corneum, clearer epidermal layers, and markedly reduced epidermal thickening, almost restoring it to the initial state. This performance showed a significant difference compared to pure CA. The superior repair effect is likely due to the encapsulated madecassoside enhancing the reparative effect of CA, resulting in excellent repair efficacy.

The cornified envelope (CE) is the envelope of corneocytes, providing a highly flexible structure and correct binding sites for intercellular lipids. CE is formed by the cross-linking of various proteins, including involucrin, LOR, and filaggrin (FLG). LOR constitutes about 70% of the CE and is a major protein component found in terminally differentiated epidermal cells. It acts as a scaffold during CE formation in the epidermis, synthesized in the spinous layer and cross-linked with granular layer cells under the action of transglutaminase, forming a crucial structural support for the skin barrier. Studies have shown that LOR expression differs in the lesions of atopic dermatitis (AD) patients compared to normal skin tissue, which is related to skin barrier dysfunction [20–22]. Immunofluorescence technology is based on the antigen-antibody reaction principle. A known LOR antibody is first labeled with a fluorophore. This fluorescent antibody then acts as a probe to bind to the corresponding LOR antigen within cells or tissues [23,24].

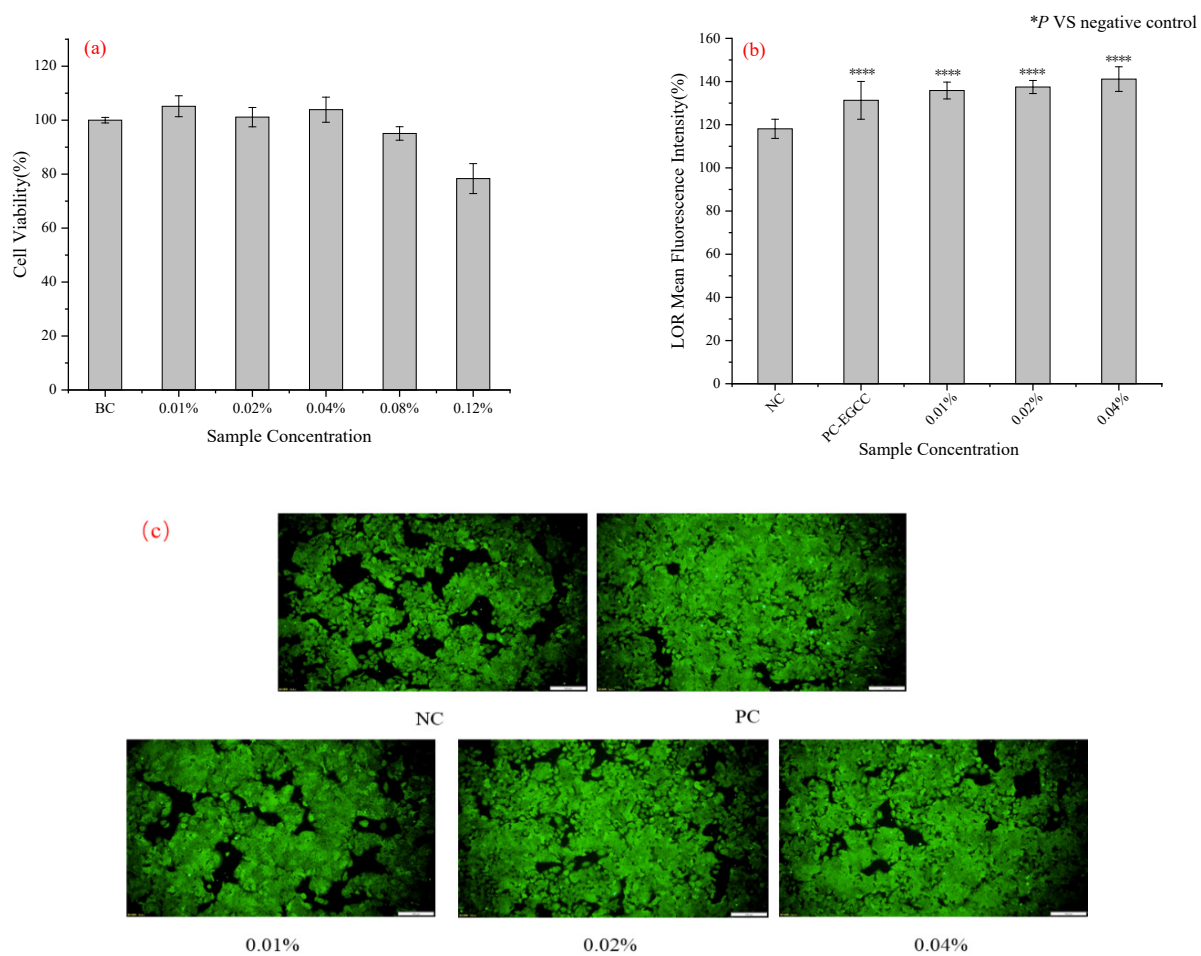


Figure 9. Effect of different concentrations of CCME on LOR expression: (a) Cytotoxicity tolerance in HaCaT cells (MTT assay), (b) Impact on LOR expression in HaCaT cells, (c) Fluorescence staining images of LOR expression.

To further analyze the effect of CCME on epidermal differentiation, tissues treated with CCME were subjected to immunohistochemistry using a LOR antibody. Based on the MTT results (Figure 9a), no significant cytotoxicity was observed at concentrations of 0.01%, 0.02%, and 0.04% (w/v%), so these concentrations were selected for subsequent experiments. Compared to the negative control (MEM medium), the positive control (EGCG) significantly upregulated LOR expression in HaCaT cells, confirming the validity of the assay model. Fluorescence microscopy visualized the location and intensity of fluorescence, indicating the nature, localization, and level (upregulation/downregulation) of the antigen or antibody. Brighter LOR mean fluorescence intensity (MFI) images indicated higher values and stronger barrier repair function. LOR expression

showed an increasing trend with concentration (Figure 9b). Concentrations of 0.01%, 0.02%, and 0.04% (w/v%) CCME significantly upregulated LOR expression in HaCaT cells, with MFI values of $135.844 \pm 3.904\%$, $137.455 \pm 3.035\%$, and $141.131 \pm 5.682\%$, respectively. Increasing LOR expression levels in keratinocytes activates and promotes epidermal cell differentiation, thereby demonstrating the repair effect.

4. Discussion

CA is a high-quality plant oil containing multiple bioactive compounds with diverse skincare benefits. The oleic acid in CA shares structural similarity with the primary components of human sebum, granting it exceptional skin affinity [2]. Rich in bioactive substances such as vitamin E and tea polyphenols, CA enhances skin elasticity, boosts barrier resilience, delays aging signs, and reduces stretch marks [2,4]. As CA incorporation levels increase in cosmetic formulations, its limitations particularly poor thermal stability and susceptibility to oxidation have become apparent [3,25]. Addressing these bioavailability challenges would significantly expand its applications. Currently, most CA-containing skincare products are oil-based formulations. W/O microemulsions, characterized by their clear, transparent appearance, offer distinct advantages: they maintain visual homogeneity when incorporated into final products and serve as effective topical delivery systems. In this study, we engineered a W/O CCME incorporating water-soluble synergistic actives to enhance its functional value.

In this study, surfactant selection and the Smix ratio critically influenced the microemulsion region in the phase diagram. Employing soybean lecithin and DPG as emulsifiers proved essential for forming a thermodynamically stable system [11,12]. Although microemulsions typically self-assemble spontaneously, the energy input required here (heating/stirring) suggests nanoemulsion like behavior. Nevertheless, the sub-100 nm particle size (68.96 ± 2.91 nm), low polydispersity index (0.267 ± 0.015), and negative zeta potential (-13.62 mV) align with characteristics of stable microemulsions used in cosmetics [8,26]. The exceptional centrifugal stability ($KE < 5\%$) and long-term storage stability (8 weeks at $4\text{--}45^\circ\text{C}$) can be attributed to steric stabilization provided by lecithin's bilayer structure, coupled with DPG's cosurfactant role in reducing interfacial tension [12]. The slight particle size increase at 4°C (68.96 nm to 92.64 nm) likely relates to phospholipid phase transitions but causes no macroscopic instability—demonstrating optimized low-temperature stability compared to pure camellia seed oil.

The CCME developed in this study exhibits nanoscale dimensions, which combined with lipid fluidization effects on the stratum corneum, confers exceptional penetration properties. The unique compartmentalization of the microemulsion simultaneously protects labile compounds from degradation and enables synchronized delivery of active ingredients to keratinocytes [26,27]. In vitro studies confirmed that this lecithin-based W/O nano-carrier co-encapsulating hydrophilic actives (*Camellia japonica* extract and madecassoside) synergistically enhances skin barrier repair functions—a key advancement validated through both 3D epidermal models and molecular assays. This is exemplified by the dose-dependent upregulation of LOR, a cornerstone structural protein constituting >70% of the cornified envelope, treatment with 0.04% CCME elevated LOR expression to 141.1% in HaCaT cells ($P < 0.01$ vs CA), directly correlating with the observed restoration of stratum corneum density in SLS-damaged tissue. Mechanistically, this enhancement likely stems from dual ligand-receptor activation: madecassoside in the aqueous core activates the AhR/OVOL1 differentiation pathway, effects potentiated by the nanocarrier's ability to co-localize these hydrophilic and lipophilic actives within the same cellular microenvironment [24].

Collectively, this multifunctional reparative platform demonstrates that rational microemulsion design transcends mere solubility improvement, instead enabling targeted release of actives that regulate molecular checkpoints of epidermal barrier homeostasis. While clinical studies and formulation applications remain unexplored, future work should validate these findings *in vivo* to substantiate cosmetic applications.

5. Conclusions

This study addressed the bottlenecks of Camellia seed oil (CA) in cosmetic applications—susceptibility to oxidation, potential precipitation at low temperatures, and low transdermal absorption—by innovatively employing a water-in-oil microemulsion technology. The optimal formulation was determined through pseudo-ternary phase diagram optimization: using soybean lecithin and dipropylene glycol ($K_m = 2.5:1$) as the composite emulsifier, and combining CA with hydrophilic active components (*Camellia japonica* flower extract and madecassoside = 5:1) at an oil phase-to-emulsifier ratio of 5:5. This successfully yielded a CCME with stable physicochemical properties. Characterization revealed a homogeneous spherical structure with an average particle size of 68.96 ± 2.91 nm, a PDI of 0.267 ± 0.015 , and a zeta potential of -13.62 ± 0.57 mV. The CCME maintained structural stability under centrifugation (4000 rpm for 40 minutes) and 8 weeks of temperature-variation storage ($4\text{--}45^\circ\text{C}$), showing no phase separation or aggregation. Efficacy validation demonstrated that the nano-carrier system significantly enhanced active permeation. Franz diffusion cell tests and human confocal Raman spectroscopy

confirmed a cumulative permeation rate of 12.02% after 12 hours, far superior to pure CA. Simultaneously, synergistic effects boosted the DPPH radical scavenging rate to 88.25%, attributed to the synergistic antioxidant mechanism between *Camellia japonica* polyphenols and CA. Regarding skin barrier repair, the 3D epidermal model confirmed that CCME restored the densification level of the SLS-damaged stratum corneum to normal. Cell experiments further revealed that CCME concentration-dependently upregulated the expression of LOR, a key epidermal differentiation protein, elucidating the molecular mechanism underlying its promotion of barrier repair. In summary, this composite microemulsion system effectively overcomes the application limitations of CA through nano-carrier technology, achieving efficient co-delivery of active ingredients and functional synergy, providing a theoretical basis and technical pathway for developing multifunctional skincare products.

References

- [1] Huang, R. L. Chinese camellia oil (Second Edition). Beijing: China Forestry Publishing House. 2008.
- [2] Guo, J. J.; Luo J.; Liu, H. H.; Jin, D. C. Active components and skin care properties of tea seed oil from *camellia sinensis*. *BioResources*. 2024, 19, 7166-7182. [doi: 10.15376/biores.19.4.7166-7182]
- [3] Salinero, C.; Feás, X.; Mansilla, J. P.; Seijas, J. A.; Vázquez-Tato, M. P.; Vela, P.; Sainz, M. J. ¹H-nuclear magnetic resonance analysis of the triacyl glyceride composition of cold-pressed oil from *Camellia japonica*. *Molecules*. 2012, 17, 6716-6727.
- [4] Jeon, H.; Kim, J. Y.; Choi, J. K.; Han, E.; Song, C.; Lee, J.; Cho, Y. S. Effects of the extracts from fruit and stem of *camellia japonica* on induced pluripotency and wound healing. *J. Clin. Med.* 2018, 7, 449.
- [5] Jung, E.; Lee, J.; Beak, J.; Jung, K.; Lee, J.; Huh, S.; Kim, S.; Koh, J.; Park, D. Effect of *camellia japonica* oil on human type I procollagen production and skin barrier function. *J. Ethnopharmacol.* 2007, 112, 127-131.
- [6] Zhu, M.; Jing, R. S. Preparation and Activity study of antioxidant camellia moisturizing oil. *J. Hefei Univ. Technol.* 2019, 42, 273-277.
- [7] Piao, M. J.; Yoo, E. S.; Koh, Y. S.; Kang, H. K.; Kim, J.; Kim, Y. J.; Kang, H. H.; Hyun, J. W. Antioxidant effects of the ethanol extract from flower of *camellia japonica* via scavenging of reactive oxygen species and induction of antioxidant enzymes. *Int. J. Mol. Sci.* 2011, 12, 2618-2630.
- [8] Lawrence, M. J.; Gees, G. D. Microemulsion-based media as novel drug delivery systems. *Adv. Drug Deliv. Rev.* 2000, 45, 89-121.
- [9] Li, L. F.; Qu, J. P.; Liu, W. D.; Peng, B. L.; Cong, S. N.; Yu, H. B.; Zhang, B.; Li, Y. Y. Advancements in characterization techniques for microemulsions: from molecular insights to macroscopic phenomena. *Molecules*. 2024, 29, 2901.
- [10] Tsai, M. J.; Chang, W. Y.; Chiu, I. H.; Lin, I. L.; Wu, P. C. Improvement in Skin Penetration Capacity of Linalool by Using Microemulsion as a Delivery Carrier: Formulation Optimization and In Vitro Evaluation. *Pharmaceutics*. 2023, 15, 1446.
- [11] Lu, T. M. T.; Huynh, K. D.; Nguyen, M. D. Applications of lecithin in emulsion stabilization and advanced delivery systems in cosmetics: A mini-review. *Results Surf. Interfaces*. 2025, 19, 100543.
- [12] Pearson, R. H.; Pascher I. The molecular structure of lecithin dihydrate. *Nature*. 1979, 281, 499-501.
- [13] Moghandam, S. H.; Saliaj, E.; Wettig, S. D.; Dong, C.; Ivanova, M. V.; Huzil, J. T.; Foldvari, M. Effect of chemical permeation enhancers on stratum corneum barrier lipid organizational structure and interferon alpha permeability. *Mol. Pharm.* 2013, 10, 2248-2260.
- [14] Almgren, M. Mixed micelles and other structures in the solubilization of bilayer lipid membranes by surfactants. *Colloids Surf. B Biointerfaces*. 2000, 1508, 146-163.
- [15] Callender, S. P.; Mathews, J. A.; Kobernyk, K.; Wettig, S. D. Microemulsion utility in pharmaceuticals: Implications for multi-drug delivery. *Int. J. Pharm.* 2017, 526, 425-442.
- [16] Okur, N. U.; Yavasoğlu, Y.; Karasulu, H. Y. Preparation and evaluation of microemulsion formulations of naproxen for dermal delivery. *Chem. Pharm. Bull.* 2014, 62, 135-143.
- [17] Blois, M. S. Antioxidant determination by the use of a stable free radical. *Nature*. 1958, 181, 1199-1200.
- [18] Caddeo, C.; Manconi, M.; Fadda, A. M.; Lai, F.; Lampis, S.; Díez-Sales, O.; Sinico, C. Nanocarriers for antioxidant resveratrol: Formulation approach vesicle self-assembly and stability evaluation. *Colloids Surf. B Biointerfaces*. 2013, 111, 327-332.
- [19] Hwang, J. H.; Jeong, H.; Lee, N.; Hur, S.; Lee, N.; Han, J. J.; Jang, H. W.; Choi, W. K.; Nam, K. T.; Lim, K. M. Ex vivo live full-thickness porcine skin model as a versatile in vitro testing method for skin barrier research. *Int. J. Mol. Sci.* 2021, 22, 657.
- [20] Jung, Y. O.; Jeong, H.; Cho, Y.; Lee, E. O.; Jang, H. W.; Kim, J.; Nam, K.; Lim, K. M. Lysates of a probiotic, *Lactobacillus rhamnosus*, Can improve skin barrier function in a reconstructed human epidermis model. *Int. J. Mol. Sci.* 2019,

20, 4289.

- [21] Akiyama, M. The roles of ABCA12 in epidermal lipid barrier formation and keratinocyte differentiation. *Biochim. Biophys. Acta.* 2014, 1841, 4435-440.
- [22] Jing, C. X.; Guo, J. L.; Li, Z. Z.; Xu, X. H.; Wang, J.; Zhai, L.; Liu, J. Z.; Sun, G.; Wang, F.; Xu, Y. F. Screening and research on skin barrier damage protective efficacy of different mannosylerythritol lipids. *Molecules.* 2022, 27, 4648.
- [23] Sun, W.; He, J.; Zhang, Y. H.; He, R. K.; Zhang, X. G. Comprehensive functional evaluation of a novel collagen for the skin protection in human fibroblasts and keratinocytes. *Biosci. Biotechnol. Biochem.* 2023, 87, 724-735.
- [24] Hashimoto-Hachiya, A.; Tsuji, G.; Murai, M.; Yan, X. H.; Furue, M. Upregulation of FLG, LOR, and IVL expression by Rhodiola crenulata root extract via aryl hydrocarbon receptor: differential involvement of OVOL1. *Int. J. Mol. Sci.* 2018, 19, 1654.
- [25] Chaiyana, W.; Leelapornpisid, P.; Jakmunee, J.; Korsamphan, C. Antioxidant and Moisturizing Effect of Camellia assamica Seed Oil and Its Development into Microemulsion. *Cosmetics.* 2018, 5, 40.
- [26] El Maghraby, G.M. Transdermal delivery of hydrocortisone from eucalyptus oil microemulsion: Effects of cosurfactants. *Int. J. Pharm.* 2008, 355, 285–292.
- [27] Trotta, M.; Ugazio, E.; Gasco, M. R. Pseudo-ternary phase diagrams of lecithin-based microemulsions: Influence of monoalkylphosphates. *J. Pharm. Pharmacol.* 1995, 47, 451–454.